Stepwise frequency tuning of a gyrotron backward-wave oscillator

T. H. Chang
Department of Physics, National Tsing Hua University, Hsinchu, Taiwan

S. H. Chen
Department of Physics, National Changhua University of Education, Changhua, Taiwan

(Received 15 July 2004; accepted 6 October 2004; published online 14 December 2004)

The gyrotron backward-wave oscillator (gyro-BWO) features broadband tunability, but ragged tuning curves are frequently observed experimentally. Accordingly, a Ka-band gyro-BWO experiment with external circuit mismatch was conducted to examine its tuning properties at two reflected strengths: one is slightly mismatched (15 dB reflection) and the other can be categorized as matched (30 dB reflection). Stepwise frequency tunings by varying the magnetic field, the beam voltage, and the beam current were observed under mismatched conditions. A self-locking model was introduced using the concept of injection-locking, where the output and reinjected signals tend to form a stable phase relation, favoring certain discrete oscillation frequencies. The observed frequencies agree closely with the calculated frequencies. Smooth tuning curves were also obtained, revealing a remedy for the stepwise tuning of a gyro-BWO. © *2005 American Institute of Physics*. [DOI: 10.1063/1.1827217]

I. INTRODUCTION

Among gyrotron oscillators, the gyrotron backward-wave oscillator (gyro-BWO) exhibits superior frequency tunability. The oscillation formed by an internal feedback loop is composed of a forward-moving electron beam and a backward-propagating wave. Figure 1 plots the ω-k_z diagram of the gyro-BWO. The parabola is the dispersion relation of the waveguide mode and the oblique line is the beam-wave resonant line. Varying the magnetic field B_0 or the beam voltage V_b changes their intersection, and therefore the operating conditions. Smooth variations in the frequency and output power are theoretically predicted. However, ragged[1–3] or even piecewise discontinuous[4,5] tuning curves have been observed in most of the gyro-BWO experiments.

Multimode competition, single-mode self-modulation, and circuit reflection are the three major causes of the ragged frequency tuning in the gyro-BWO. The competition among different axial modes ($\ell=1,2,3,\ldots$) of the operating TE_{11} mode with fundamental cyclotron harmonic ($s=1$) is typically more critical than that among various transverse modes (TE_{mn}) with higher cyclotron harmonics ($s\geqslant 2$).[6] Each axial mode has its distinct field profile and electron transit angle at the onset stage.[7] All the field profiles are similar at the saturated phase because of the nonlinear field contraction,[8] which thus increases the possibility of the axial mode competition.[9–11]

The self-modulation is caused by overdriving a single mode. Recent investigations reveal that self-modulation normally takes place at a beam current that is several times higher than the starting current for the gyromonotron; the gyro-BWO has a much broader stationary operating regime.[12–14] Shortening the interaction length has been demonstrated to effectively minimize the probability of mode competition and considerably increasing the threshold current for nonstationary behavior.[8] It effectively alleviates the threat of unsmooth tuning by the two aforementioned mechanisms. One issue that remains to be examined is the effect of external circuit reflection.

End reflection originates from various sources, such as structural nonuniformity, window mismatch, and the mismatch of the external circuit. The reflected signal is reinjected into the interaction section to modify the oscillation condition.[15] The reinjected signal and original oscillation tend to form another steady-state phase relation, in which the phase difference between these two signals is constant with time.[16–18] The phase relation favors certain frequencies of oscillation, thus resulting in stepwise tuning curves. Such a frequency pulling effect is critical to parameter-sensitive oscillation, such as gyro-BWO. The reflection-induced effect has been investigated in some high power microwave oscillators,[18–24] but works that involve the gyro-BWO are few.

A Ka-band gyro-BWO experiment was performed to examine the stepwise tuning under various operating parameters with external circuit reflection. A simplified self-locking model is introduced to elucidate the physical causes of the stepwise frequency tuning. The rest of this paper is organized as follows. Section II describes the experimental setup. Section III proposes a self-locking model. Section IV presents the experimental observations, which are compared with the calculated results. Section V summarizes this work and provides suggestions for future studies.

II. EXPERIMENTAL SETUP

Figure 2 schematically depicts the investigated Ka-band gyro-BWO. A magnetron injection gun generates the electron beam. The applied beam voltage V_b extracts and accelerates the electrons, which then propagate along the magnetic field through the magnetic compression in the drift region. At the entry of the interaction section, the beam parameters are estimated as the velocity spread ($\Delta v_z/v_z$) of $\approx$5% and the pitch angle α of 0.8–1.1. The interaction sec-

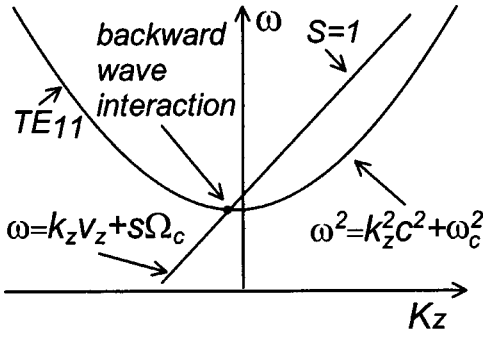

FIG. 1. The ω-k_z diagram of a waveguide mode (parabola) and the beam-wave resonant line (oblique line) with fundamental cyclotron harmonics ($s=1$). The waveguide mode is TE_{11}. The intersection, the resonant point, falls in the backward regime ($k_z \leqslant 0$) of gyro-BWO. The operating points can be adjusted by changing the magnetic field, the beam voltage, or the beam current.

tion is entirely immersed in a uniform magnetic field B_0 provided by a superconducting magnet. After the interaction, the spent electron beam is dumped onto the collector, where the collected electrons are measured as the beam current I_b. The beam current is kept as a constant of 4 A for both the magnetic field B_0 tuning and the beam voltage V_b tuning. The magnetic field and the beam voltage are maintained at 14.6 kG and 100 kV, respectively, for the beam current tuning.

The interaction section consists of a uniform length of 30 mm and a radius of 2.68 mm; both ends are connected via slightly asymmetric tapered sections with lengths 35 mm (upstream) and 40 mm (downstream) to a short straight section with a radius of 3.175 mm. The magnetic field in the upstream taper section is also slightly up-tapered. Both the waveguide tapering and the magnetic field tapering not only enhance the interaction efficiency of gyro-BWO, but eliminate the possible mode competition. The upstream taper section also functions as a mode and polarization converter[25] of the circularly polarized TE_{11} wave back into a linearly polarized TE_{11} wave in the cylindrical waveguide. It then couples the wave out from a hole on the wall of the cylindrical waveguide with a TE_{10} mode in the rectangular waveguide for further diagnosis. Both forward and backward waves are transmitted through a WR-28 waveguide of length L 89.6 mm, as shown in the Fig. 2.

To explore the effect of the external reflection, an artificial circuit mismatch is introduced to produce wave reflection and, thereby, elucidate the effect of the external reflection. The dominant output power is associated with a backward wave for the gyro-BWO. The circuit mismatch (an iris) is placed near the end of the room-temperature bore of the superconducting magnet for the backward-wave signal but not for the forward-wave signal. Two reflected strengths, 15 dB and 30 dB are applied: the former represents relatively poor matching while the latter represents a good matching. A severe reflection, which might be responsible for some complicated behavior or even chaotic behavior, is beyond the scope of this work. The diagnostic system includes a power detecting unit and a frequency meter. The output power is detected using a well-calibrated crystal detector (with an estimated accuracy of ±5%) and the frequency is measured using a precision frequency meter (with resolution of 5 MHz).

III. SELF-LOCKING MODEL

The injection locking technique is commonly used in phase and amplitude control over a free-running oscillator. It involves injecting an external signal of frequency ω_1 into an oscillator of resonant frequency ω_0. When the free-running oscillator is locked by an externally injected signal, the oscillation frequency is determined exactly by the frequency of the external signal ω_1. The resultant amplitude V and the phase difference ϕ between the injected and locked signals depend on some factors, such as the initial frequency separation $(\omega_0 - \omega_1)$, the ratio of the injected power and the original oscillating power, and the quality factor of the oscillator.

Figure 3(a) shows the schematic diagram of an injection locking model using an effective lump circuit. The effect of electromagnetic resonance is expressed in terms of the capacitance C_{eff} and inductance L_{eff}. The conductance G_{eff} represents the effective total power loss, including ohmic and diffraction losses. The negative conductance of G_{m} implies that the medium, the electron beam, can generate, rather than dissipate, a wave. Assume the injected signal (with subindex 1) and output signal can be expressed as follows:

$$v_1 = V_1 e^{j\omega_1 t}, \quad v = V e^{j\omega_0 t + j\phi}, \tag{1}$$

where V_1 and V are amplitudes. Substituting Eq. (1) into Kirchhoff's loop rule and decomposing the real and imaginary parts, yields the following phase relation:

$$\frac{d\phi}{dt} + (\omega_1 - \omega_0) = \frac{\omega_0}{Q}\frac{V_1}{V}\sin\phi, \tag{2}$$

where Q is the quality factor.

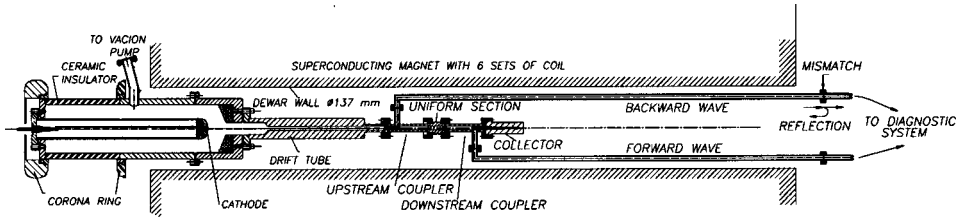

FIG. 2. The schematic diagram depicts the experimental configuration of a Ka-band gyro-BWO. The entire tube is placed in the bore of a superconducting magnet. The electron beam is generated by a magnetron injection gun. Both forward and backward waves are extracted for further diagnosis. An artificial circuit mismatch is applied to generate a reflection.

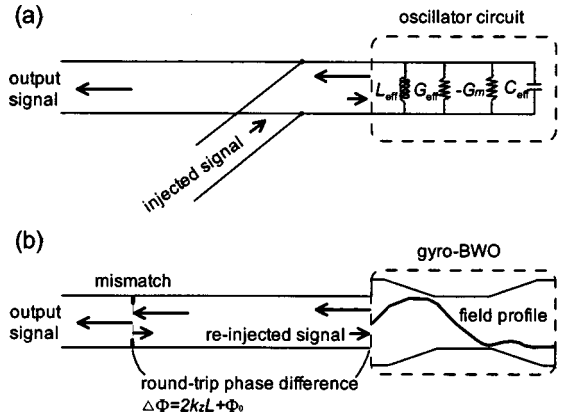

FIG. 3. (a) An injection locking model in which the oscillation is expressed as an effective lump circuit. (b) A self-locking model in which the phase relation between the output signal and the reinjected signal is shown. The interaction structure of the oscillator and a representative field profile are also displayed as a reference.

This study adapts the above concept to the condition of interests by treating the reflected signal as an injected one. Figure 3(b) schematically depicts the self-locking effect under study. A reflected signal is usually caused by the external circuit mismatch. Under steady-state operation, the phase difference ϕ must be constant in time and the resonant frequencies are the same ω_0. Analyzing Eq. (2) yields the phase difference ϕ of $2m\pi$, where m is the integer. This study is concerned only with the steady-state condition. A much more comprehensive time-dependent model can be found in Ref. 18. Therefore, the round-trip phase difference ϕ can be expressed as

$$\phi = \frac{2\pi}{\lambda_g} 2L + \phi_0 = \frac{4\pi L}{c}\sqrt{(f^2 - f_c^2)} + \phi_0, \tag{3}$$

where λ_g, L, c, and f_c are the guided wavelength, the external circuit length, the speed of light, and the cutoff frequency of the waveguide, respectively. Notably, the phase constant ϕ_0 is determined by the boundary conditions and only slightly influences the resonant frequency. For convenience, ϕ_0 is set to zero.

The phase relation indicates that certain frequencies are favored. These are

$$f_m = \sqrt{f_c^2 + \left(\frac{m}{2}\right)^2 \left(\frac{c}{L}\right)^2}, \tag{4}$$

where m is a positive integer and f_m is mth preferred frequency. The favoring of some particular frequencies reveals that the oscillation may be stuck in a particular mode. The following experimental results further demonstrate this effect.

IV. RESULTS AND DISCUSSION

A. Magnetic field tuning

Figure 4 shows the tunability of the magnetic field for two different circuit reflections. The beam current and voltage are 4 A and 100 kV, respectively. Figure 4(a) plots the output power versus the magnetic field, while Fig. 4(b) shows the oscillation frequency vs the magnetic field. The maximum output power is 106 kW, corresponding to an efficiency of 26%. For a 15 dB reflection (dashed lines with empty squares), the output power and oscillation frequency both exhibit zigzag tuning curves as the magnetic field is increased from 14.1 to 14.7 kG. This effect is apparently alleviated when the reflection is reduced to a much lower value of 30 dB (solid lines with filled circles).

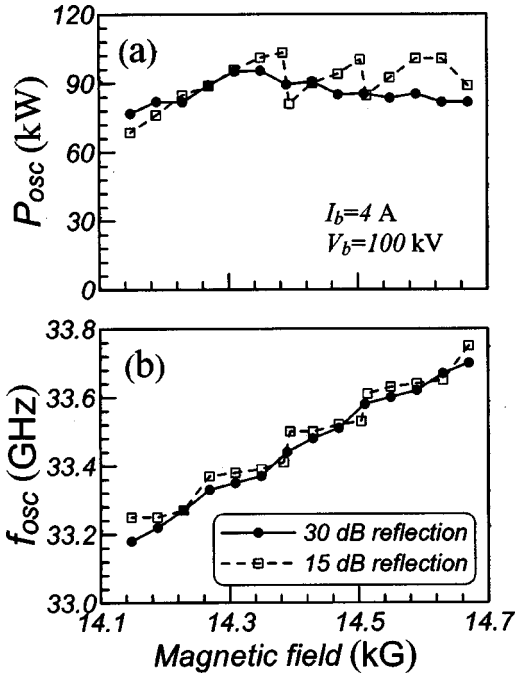

FIG. 4. Output power and oscillation frequency vs the magnetic field in the cases of poor matching (15 dB, dashed lines with empty squares) and good matching (30 dB, solid lines with filled circles), respectively. The beam current is 4 A and the beam voltage is 100 kV.

B. Beam voltage tuning

Figure 5 illustrates the output power and oscillation frequency versus the operating beam voltage. The beam voltage is varied from 80 kV to 100 kV, while the beam current and the magnetic field are fixed at 4 A and 14.6 kG, respectively. Figures 5(a) and 5(b) plot the power and frequency versus the beam voltage, respectively. The maximum efficiency is 26%. As in Fig. 4, the amplitude of reflection determines the smoothness of the tuning curves. Reducing the reflection from 15 dB (dashed lines with empty squares) to 30 dB (solid lines with filled circles) is to smoothen the tuning of both power and frequency.

C. Beam current tuning

Altering the beam current can modify the interaction dynamics and subsequently detune the oscillation frequency. The presence of the electron beam modifies the effective dielectric constant, leading to an up shift in resonant frequency.[26] This effect is particularly evident for a parameter-sensitive oscillation, e.g., the gyro-BWO. Although the current tuning is not a common means of adjusting the resonant frequency, this result still can be used to

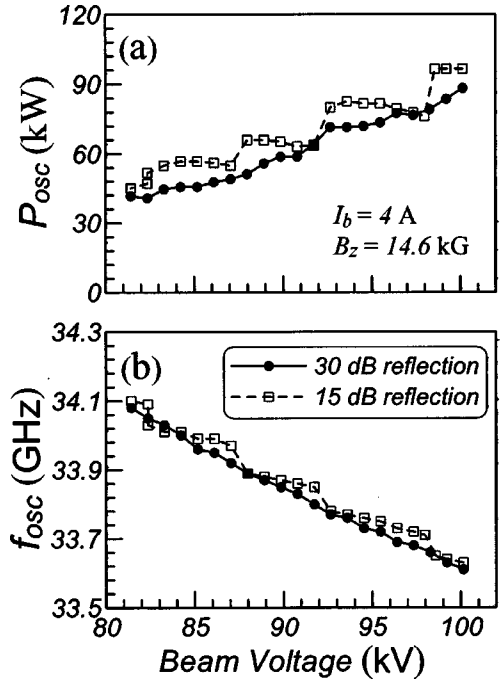

FIG. 5. Output power and oscillation frequency vs the operating beam voltage in the cases of poor matching (15 dB, dashed lines with empty squares) and good matching (30 dB, solid lines with filled circles), respectively. The beam current is 4 A and the magnetic field is 14.6 kG.

elucidate the stepwise tuning effect. Figure 6 displays the tuning of the beam current while the beam voltage and the magnetic field are kept at 100 kV and 14.6 kG, respectively. The beam current is increased from the start-oscillation current of 0.95 A to a maximum value of 6 A. Figures 6(a) and 6(b) plot the output power and oscillation frequency versus the beam current, respectively. As in Figs. 4 and 5, stepwise frequency tuning is observed in the circuit with a reflection of 15 dB. When the circuit reflection is reduced to 30 dB, the power and frequency tuning curves (solid lines with filled circles) are smoother than at 15 dB.

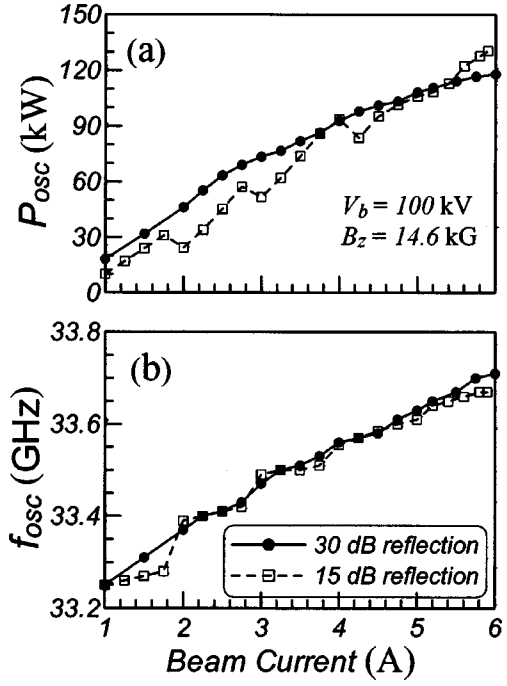

FIG. 6. Output power and oscillation frequency vs the operating beam current in the cases of poor matching (15 dB, dashed lines with empty squares) and good matching (30 dB, solid lines with filled circles). The beam voltage and the magnetic field are 100 kV and 14.6 kG, respectively.

TABLE I. Calculated and measured frequencies against the magnetic field, the beam voltage, and the beam current tunings. The calculated frequencies are obtained from Eq. (4) with length $L=89.6$ cm and $m=154-160$. The measured frequencies are taken at the maximum output power of each mode, except in the case of beam current tuning where the frequencies are measured in the middle of each step. The symbol "-" indicates that the value was unavailable.

Self-locking model (calculated)	Magnetic field tuning (measured)	Beam voltage tuning (measured)	Beam current tuning (measured)
33.252 ($m=154$)	33.27	-	33.26
33.382 ($m=155$)	33.41	-	33.41
33.512 ($m=156$)	33.53	-	33.50
33.643 ($m=157$)	33.64	33.64	-
33.774 ($m=158$)	-	33.77	-
33.905 ($m=159$)	-	33.88	-
34.036 ($m=160$)	-	34.00	-

Table I summarizes the calculated and measured frequencies. The calculated frequencies are obtained from Eq. (4) with the length L of 89.6 cm and index m from 154 to 160. The frequencies are measured at the maximum output power of each mode, except in the case of beam current tuning, in which the frequencies are measured in the middle of each step. Interestingly, reducing the reflection does not alter the frequency separation, but effectively minimizes the stepwise tuning effect. The calculated and measured frequencies of the three tunings are consistent with each other.

Like the stepwise operating frequencies, the output power also exhibits a zigzag tuning characteristic. Such effects are qualitatively specified as follows. The reflected power can be regarded as a reinjected signal, so the overall output power is slightly enhanced, just as in the case of the injection locking. Greater injected power corresponds to the more output power. Hence, the total output power with high reflection (15 dB) is normally exceeds that with low reflection (30 dB). As the operating parameters are changed, the oscillation signal and reinjected signal are not always in synchronization, resulting in the phase mismatch and ragged tuning.

V. CONCLUSIONS

The work demonstrates that the reflection is responsible for the stepwise frequency tuning, even in the absence of mode competition and self-modulation. This effect was especially evident for a parameter-dependent oscillation, such as gyro-BWO.

The results predicted by the self-locking model are consistent with the experimental results. The rippled output power and piecewise oscillation frequencies of magnetic field, beam voltage, and beam current tunings could be rem-

edied by simply reducing the reflection down to a value of 30 dB. The excellent agreement as shown in Table I provides a preliminary physical explanation for the ragged tuning caused by the external reflections. A more thorough theoretical study is being performed.

The fact that the oscillation frequency is sensitive to the external reflection reveals that the operation of gyro-BWO depends strongly on the dynamics of the operating parameters. Understanding this characteristic helps us to achieve smooth tunings and to realize the advantage of the broadband frequency tunability of gyro-BWO. However, some phenomena demand further explanation, e.g., the stability during mode transition *m* and nonstationary behavior due to heavy reflection. These phenomena suggest areas that require further numerical and experimental studies.

ACKNOWLEDGMENTS

Professor K. R. Chu, Dr. F. S. Cheng, and C. C. Chiu are appreciated for numerous helpful discussions and technical supports.

The authors would like to thank the National Science Council of the Republic of China, Taiwan, for financially supporting this research under Contract No. NSC92-2119-M-007-053.

[1] S. Y. Park, R. H. Kyser, C. M. Armstrong, R. K. Parker, and V. L. Granatstein, IEEE Trans. Plasma Sci. **18**, 321 (1990).
[2] C. S. Kou, S. H. Chen, L. R. Barnett, H. Y. Chen, and K. R. Chu, Phys. Rev. Lett. **70**, 924 (1993).
[3] T. A. Spenser, C. E. Davis, K. L. Hendrics, F. J. Agee, and R. M. Gilgenbach, IEEE Trans. Plasma Sci. **24**, 630 (1996).
[4] M. A. Basten, W. C. Guss, K. E. Kreischer, R. J. Temkin, and M. Caplan, Int. J. Infrared Millim. Waves **16**, 889 (1995).
[5] K. Kamada, K. Nawashiro, F. Tamagawa, H. Igarashi, S. Kizu, C. Y. Lee, S. Kawasaki, R. Ando, and M. Masuzaki, Int. J. Infrared Millim. Waves **19**, 1317 (1998).
[6] Y. S. Yeh, T. H. Chang, and T. S. Wu, Phys. Plasmas **11**, 4547, (2004).
[7] S. H. Chen, T. H. Chang, K. F. Pao, C. T. Fan, and K. R. Chu, Phys. Rev. Lett. **89**, 268303 (2002).
[8] S. H. Chen, K. R. Chu, and T. H. Chang, Phys. Rev. Lett. **85**, 2633 (2000).
[9] G. S. Nusinovich, IEEE Trans. Plasma Sci. **27**, 313 (1999).
[10] A. K. Ganguly and S. Ahn, Int. J. Electron. **67**, 261 (1989).
[11] G. S. Nusinovich and Y. P. Bliokh, Phys. Plasmas **7**, 1294 (2000).
[12] T. H. Chang, S. H. Chen, L. R. Barnett, and K. R. Chu, Phys. Rev. Lett. **87**, 064802 (2001).
[13] G. S. Nusinovich, A. N. Vlasov, and T. M. Antonsen, Jr., Phys. Rev. Lett. **87**, 218301 (2001).
[14] A. Grudiev and K. Schunemann, IEEE Trans. Plasma Sci. **30**, 851 (2002).
[15] C. S. Kou, Phys. Plasmas **1**, 3093 (1994).
[16] B. van der Pol, Philos. Mag. **3**, 65 (1927).
[17] M. E. Read, R. Seeley, and W. M. Manheimer, IEEE Trans. Plasma Sci. **13**, 398 (1985).
[18] T. M. Antonsen, Jr., S. Y. Cai, and G. S. Nusinovich, Phys. Fluids B **4**, 4131 (1992).
[19] B. Lebush, T. M. Antonsen, Jr., A. Bromborsky, W. R. Lou, and Y. Carmel, IEEE Trans. Plasma Sci. **30**, 263 (1992).
[20] Y. Choyal and K. P. Maheshwari, Phys. Plasmas **2**, 319 (1995).
[21] D. M. Goebel, E. S. Ponti, R. L. Eisenhart, and R. W. Lemke, Phys. Plasmas **6**, 2319 (1999).
[22] G. S. Nusinovich and Y. P. Bliokh, Phys. Plasmas **7**, 1294 (2000).
[23] O. Dumbrajs, M. Y. Glyavin, V. E. Zapevalov, and N. A. Zavolsky, IEEE Trans. Plasma Sci. **28**, 588 (2000).
[24] A. Grudiev, J. Jelonnek, and K. Schunemann, Phys. Plasmas **8**, 2963 (2001).
[25] T. H. Chang, L. R. Barnett, K. R. Chu, F. Tai, and C. L. Hsu, Rev. Sci. Instrum. **70**, 1530 (1999).
[26] K. R. Chu, D. S. Furuno, N. C. Luhmann, D. B. McDermott, P. Vitello, and K. Ko, IEEE Trans. Plasma Sci. **13**, 435 (1985).